Proceedings of the 2006 IEEE International Conference on Robotics and Automation
Orlando, Florida - May 2006

Sideslip angles observer for vehicle guidance in sliding conditions:

Application to agricultural path tracking tasks

Roland Lenain◇, Benoit Thuilot⋆, Christophe Cariou◇, Philippe Martinet⋆
◇ Cemagref
BP50085 - 24, av. des Landais
63172 Aubière Cedex France
roland.lenain@cemagref.fr

⋆ LASMEA
24, av. des Landais
63177 Aubière Cedex France
benoit.thuilot@lasmea.univ-bpclermont.fr

***Abstract*— Automatic devices dedicated to vehicle guidance in off-road conditions are necessarily confronted with sliding phenomenon, since it may considerably damage the accuracy of the following task. Control laws taking explicitly into account such a phenomenon have already been designed in previous work. They can actually improve the guidance accuracy. However their efficiency is highly dependent on the sliding parameters estimation (since these parameters cannot be provided by a direct measurement). In this paper, an observer-like estimator is designed, providing sideslip angles from a single exteroceptive sensor, namely a Real Time Kinematic GPS (RTK-GPS). Improvements in guidance accuracy, with respect to previous estimation approaches, is demonstrated through full scale experiments, addressing agricultural applications.**

I. Introduction

The growing accuracy requirements in agricultural tasks, with respect to pollution concerns, have generated many developments in machinery dedicated to farm work. In particular, autonomously guided vehicles have appeared to be attractive since they allow to increase both repetitiveness and work accuracy (e.g. overlapping areas when spraying pesticides can be limited). In addition, the benefits of such automatic systems are also the reduction of work hardness (since the tracking task is achieved autonomously), and an improvement in safety. These numerous advantages and interests for the farmers have motivated increasing research and developments in this topic. Indeed, numerous systems are under development or have already been marketed (e.g. CLAAS [2], John Deere [8], see also [9]). Most of these devices are relying on a GPS sensor, often associated with additional exteroceptive sensors, such as INS, laser, cameras, etc. (see for instance [5] and [10]). However, these systems have been designed to perform specific tasks (harvesting [2], achieving perfectly straight runs [8], etc.) and are not able to preserve a good tracking accuracy, out of their dedicated application field. Moreover, few of them are able to take into account for sliding phenomena, despite these effects inevitably occur during agricultural tasks (especially when operating on sloping fields or when performing half turns), and considerably damage the guidance accuracy (as has been pointed out for instance in [11]).

Designing a versatile guidance control law achieving accurate path tracking, whatever the conditions of adherence and whatever the path to be followed, is our current research interest. Moreover, it is desired that the autonomous vehicle relies only on one exteroceptive sensor (in our case, an RTK-GPS). In order to describe accurately the vehicle behaviour in presence of sliding, it would be natural to rely on a dynamic model (see for instance [3]). However, such models are large and therefore not very tractable from a control point of view. Moreover, they demand the knowledge of numerous varying parameters (such as wheel/ground conditions) that could not be obtained from our sensor configuration. Therefore, extended kinematic models have appeared to be more convenient with respect to our aims. On one hand, sliding phenomena can be described by few parameters. On the other hand, the powerful path tracking control laws designed from classical kinematic models (under rolling without sliding condition) can still be used as a basis to derive more accurate control laws accounting for sliding. Last developments demonstrate the relevance of this approach. However, the on-line estimation of the sliding parameters (required in the extended control law) is still a concern. A basic estimation algorithm can lead to a satisfactory tracking accuracy, despite sliding effects, except when the vehicles meet harsh conditions.

In this paper, a convenient and reliable method for sliding parameters estimation is proposed, based on observer theory. When associated with extended control law, a path tracking accurate to within 15cm (compatible with farmers' expectations) is demonstrated, even in harsh conditions. This paper is organized as follows. Vehicle modelling in presence of sliding and control design relying on this model are first recalled but not detailed, as well as the previous algorithm used to estimate sliding parameters. Then, an observer-like estimator providing more relevant sliding parameters is described. Finally, capabilities and benefits of this observer are discussed through full-scale experiments.

II. Vehicle model and previous work

A. Notations

Vehicle modelling is based on a classical kinematic model derived under rolling without sliding assumption (such as described in [14]), completed by two parameters inherited from a dynamic consideration and consistent with sideslip angles. This model is called "extended kinematic model" and can describe vehicle motion in presence of sliding. More precisely, two sliding parameters (β_P^R and β_P^F) have been introduced. They are representative of the difference between the theoretical orientation of the speed vector at tyre centre (i.e the wheel orientation) and the actual one, as depicted on

figure 1. Notations used in this paper can also be found on this figure and are listed below:

- $\mathcal{C}$ is the path to be followed.
- O is the centre of the vehicle virtual rear wheel. It is the point to be explicitely controlled.
- M is the point on $\mathcal{C}$ which is the closest to O. M is assumed to be unique, which is realistic when the vehicle remains quite close to $\mathcal{C}$.
- s is the curvilinear coordinate of point M along $\mathcal{C}$, and $c(s)$ denotes the curvature of $\mathcal{C}$ at that point.
- y and $\tilde{\theta}$ are respectively lateral and angular deviation of the vehicle with respect to the reference path $\mathcal{C}$.
- δ is the virtual front steering angle.
- v is the vehicle linear velocity, considered here as a parameter, whose value may be time-varying during the travel of the vehicle.
- L is the vehicle wheelbase.

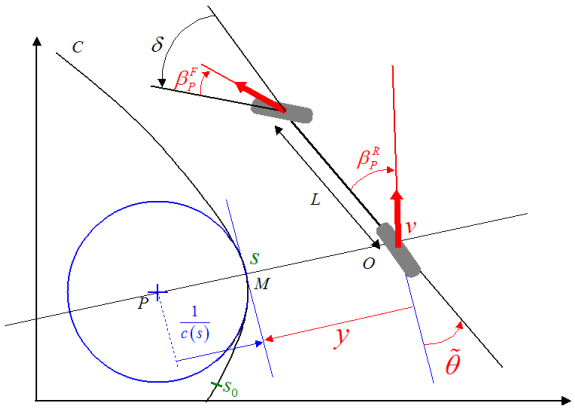

Fig. 1. Extended kinematic model parameters

B. Extended kinematic model

Assuming that the sliding phenomenon is entirely described by the introduction of the two sliding parameters (β_P^R and β_P^F), the vehicle shown on figure 1 is equivalent to a vehicle with two steering axles (as described in [7]), where the front steering angle is given by $\delta + \beta_P^F$ and the rear steering angle is given by β_P^R. Relying on these considerations, the equations of movement can be expressed by system (1).

$$\left\{ \begin{array}{rcl} \dot{s} & = & \frac{v\cos(\tilde{\theta}+\beta_P^R)}{1-c(s)y} \\ \dot{y} & = & v\sin(\tilde{\theta}+\beta_P^R) \\ \dot{\tilde{\theta}} & = & v\left[\cos\beta_P^R \frac{\tan(\delta+\beta_P^F)-\tan\beta_P^R}{L} - \frac{c(s)\cos(\tilde{\theta}+\beta_P^R)}{1-c(s)\,y}\right] \end{array} \right. \quad (1)$$

Relying on this extended kinematic model, the path tracking task aims at ensuring the convergence of lateral deviation y to zero using steering angle δ (vehicle velocity is controlled manually). As a consequence, only the last two lines of system (1) are required. This model proposes two singularities:

- $v = 0$: this singularity will not be met, since in this work, the vehicle is assumed to be always running.
- $y = \frac{1}{c(s)}$: this occurs if point O (control point) on figure 1 is superposed with the centre of curvature of the reference path. This is never the case in experiments, since the vehicle remains close to the reference path.

Finally, it can be checked that if null sliding is imposed - $(\beta_P^R, \beta_P^F) = (0, 0)$ - model (1) is equivalent to a classical car-like vehicle model under rolling without sliding assumption.

C. Description of control laws designed previously

In previous work (see [13] and [6]), several control laws have been proposed. Research work detailed in this paper is dedicated to extract sliding parameters to be introduced into control laws accounting for sliding effects, and designed from model (1). Therefore, two control laws are mentioned below and briefly described, but details are not presented.

- The first one, (called **(Control1)** below), has been designed upon a classical Ackermann model ($(\beta_P^R, \beta_p^F) = (0, 0)$). An exact linearization approach based on chained system theory has then been used. This law is particularly efficient for straight line tracking on a level ground (when sliding phenomena are indeed negligible). As soon as sliding appears (when achieving a curve or when moving on sloping fields), an important lateral deviation appears and the tracking accuracy does not meet any longer the farm tasks expectations.
- The second one, (called **(Control2)** below), takes into account for sliding, as it is based on model (1). It has been designed using both chained system theory and Model Predictive Control. It allows to preserve a good accuracy even in presence of sliding. Capabilities of this control law are satisfactory, but are very sensitive to the relevance of sliding parameters (β_P^R and β_P^F).

In the sequel of the paper, (**Control1**) will be useful to show the importance of the sliding integration into the guidance law. (**Control2**) will firstly show the improvement obtained by accounting for sliding. In a second step, this law will allow to compare the tracking results when using both estimation methods (direct calculation versus observer-like estimator).

D. Previous estimation of sliding parameters

In order to present the problematic, let us describe the material used in our application. The vehicle is an Ares 640 farm tractor, manufactured by CLAAS (shown on figure 2). It is equipped with a Real Time Kinematic GPS (Aquarius 5002 unit) supplying a position accurate to within 2cm at a 10Hz sampling frequency. Using this sensor, lateral deviation y can be directly measured, while angular deviation $\tilde{\theta}$ is estimated via Kalman filtering based on speed vector measurement, also supplied by the GPS sensor.
The two sliding parameters (β_P^R and β_P^F described on figure 1) cannot be measured directly. However, using the equations of movement (model (1)) and the numerical derivation of the measured lateral and angular deviations, one can get a system of two equations with two unknowns. As a result, sliding parameters can directly be calculated (these are checked in

Fig. 2. Experimental vehicle

practical case) by equation (2), where T is the sampling period and the superscript k denotes the k^{th} sample of a variable.

$$\begin{cases} \beta_P^R &= \arcsin\{\frac{y^k - y^{k-1}}{v.T}\} - \tilde{\theta}^k \\ \beta_P^F &= \arctan\{\frac{L}{v\cos\beta_P^R}\frac{\theta^k - \theta^{k-1}}{T} + \tan\beta_P^R\} - \delta^k \end{cases} \quad (2)$$

Unfortunately, numerical derivation of measured signals used in direct calculation (2) leads to a very noisy sliding estimation. Since it is an input of **(Control2)**, vehicle oscillations can then sometimes be recorded (especially during harsh conditions). Low-pass filters with a very low cut-off frequency are then required, but an important delay in sliding estimation is introduced. Vehicle stability is so ensured, but control law reactivity is damaged, with respect to theoretical expectations. Moreover, the estimation of the angular deviation can be biased or delayed because of the Kalman filter used for the heading evaluation and/or disturbed because of the three-dimensional effects (cabin oscillations) induced by terrain irregularities, neglected in the model. All these limitations considerably depreciate the efficiency of the sliding calculation (2) and reduce the confidence in parameters to be used in **(control2)**. These problems in the estimation of sliding parameters are therefore very harmful for the tracking accuracy. An alternative solution for the sliding parameters estimation is developed below, based on observer theory, with the aim to overcome the limitations pointed out above.

III. Observer design

A. About classical observers

Observation theory (detailed for instance in [1]) has been applied to the case of mobile robots for instance in [4] or [12]. In this last reference, observers have been designed for sideslip angles evaluation. However, this work is dedicated to tourism vehicles, which move at higher speeds than agricultural machines. Moreover, they are equipped with different and more sensors than in the application described in this paper (where an RTK-GPS is the sole exteroceptive sensor). Therefore, such classical reconstruction techniques cannot be used straightforwardly here.

Such standard observers require that parameters to be estimated belong to the state vector. In our case, sideslip angles could be added to the state vector, but no equation for their derivative is available (no analytic expression for $\dot{\beta}_P^F$ and $\dot{\beta}_P^R$ can be written with our mesurement system). Therefore, an alternative approach is proposed below.

B. Point of view used for reconstruction

The main idea is to design an observation algorithm adapted to our case by making use of the analogy between observation theory and control theory. In the approach considered in this paper, the estimation problem is viewed as a control problem. The model (1) is viewed as a process to be controlled with respect to sliding parameters (i.e. β_P^F and β_P^R are considered as control variables). The aim of the control law to be designed is then to ensure the convergence of the outputs of model (1) ($\hat{y}$ and $\hat{\tilde{\theta}}$) to the corresponding measured variables: $\bar{y}$ and $\bar{\tilde{\theta}}$, as depicted on figure 3. The Observation algorithm based on this idea is detailed below.

C. Notations for the observer design

Using the point of view described above, notations and equivalences with respect to control theory can be detailed:

- $u = \left[\beta_P^R, \beta_P^F\right]$ is viewed as the control vector of process (1).
- δ is the steering angle. In the following equations, δ is viewed as a measured parameter supplied by an angular sensor settled on the steering wheel.
- $\hat{X} = \left[\hat{y}, \hat{\tilde{\theta}}\right]$: the output of the observer. In this case, it constitutes the state vector to be controlled.
- $\bar{X} = \left[\bar{y}, \bar{\tilde{\theta}}\right]$: the measured vector (output of GPS sensor). This vector is the desired position for process (1).

The observation of sideslip angles can finally be synthesized as a classical control problem. The objective is to ensure that the state vector ($\hat{X}$ - output of the observer) converges to the desired one ($\bar{X}$ - measured output), by making use of the control variables ($\left[\beta_P^R, \beta_P^F\right]$).

Figure 3 depicts the principle of the global algorithm, where two loops are running simultaneously. First, the measured state vector $\bar{X} = \left[\bar{y}, \bar{\tilde{\theta}}\right]$ is supplied to the observer loop (at the bottom of the figure) as the desired state to be reached by the observed state. This loop achieves the estimation of the sliding parameters, which are then injected into the model used in the control loop with sliding accounted (at the top of figure 3). All parameters and variables required by the control law **(Control2)** are then addressed.

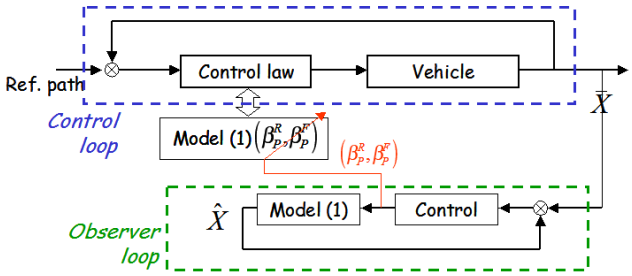

Fig. 3. Main controller and observer loops

D. Equations of the system dedicated to observation

Model (1), without curvilinear abscissa equation, is then rewritten into a non-linear state representation, given by (3)

$$\dot{\hat{X}} = f(\hat{X}, u) \quad (3)$$

where f is defined by (1) and is recalled in (4):

$$f(\hat{X},u) = \begin{cases} f_1 = v\sin(\hat{\tilde{\theta}}+u_2) \\ f_2 = v\left[\cos u_2 \frac{\tan(\delta+u_1)-\tan u_2}{L} - c(s)\frac{\cos(\hat{\tilde{\theta}}+u_2)}{1-c(s)\hat{y}}\right] \end{cases} \quad (4)$$

In order to control system (3), let us linearize this state equation with respect to "control vector" u around zero (no sliding), since sideslip angles are close to some degrees. This leads to equation (5):

$$\dot{\hat{X}} = f(\hat{X},0) + B(\hat{X})u \quad (5)$$

with B denoting the derivative of f with respect to control u:

$$B(\hat{X}) = \frac{\partial f}{\partial u}(\hat{X},0) = \begin{bmatrix} v\cos\hat{\tilde{\theta}} & 0 \\ v\frac{c(s)\sin\hat{\tilde{\theta}}}{1-c(s)\hat{y}} - \frac{v}{L} & \frac{v}{L}\left(1+\tan^2\delta\right) \end{bmatrix} \quad (6)$$

According to definition (6), matrix $B(\hat{X})$ is invertible under the condition: $\tilde{\theta} \neq \frac{\pi}{2}[\pi]$. It is met during tracking, if initialization is achieved properly.

E. Observer equation - error convergence

The convergence of $\hat{X}$ to $\bar{X}$ is classically achieved by considering the observation error (called ϵ, and defined by $\epsilon = \hat{X} - \bar{X}$). However, the equation defining the error dynamics $\dot{\epsilon}$ requires the derivation of $\bar{X}$ (measured state vector). It is however not analytically available.

To overcome this problem, the derivative of the measured state vector is introduced into the error equation via a numerical derivation, as defined by (7)

$$\dot{\bar{X}}^M = \begin{cases} \frac{\bar{X}_{[k]}-\bar{X}_{[k-1]}}{T} \\ \frac{\bar{\tilde{\theta}}_{[k]}-\bar{\tilde{\theta}}_{[k-1]}}{T} \end{cases} \quad (7)$$

The error dynamics can then be defined by equation (8):

$$\dot{\epsilon} = f(\hat{X},0) - \dot{\bar{X}}^M + Bu \quad (8)$$

The observer objective is to ensure that the error ϵ converges to zero. This can be achieved by introducing a matrix G Hurwitz and by imposing the following condition:

$$\dot{\epsilon} = G\cdot\epsilon \quad (9)$$

Since matrix $B(\hat{X})$ is invertible, condition (9) can be ensured by designing the control law (10):

$$u = B(\hat{X})^{-1}\left\{G\cdot\epsilon - f(\hat{X},0) + \dot{\bar{X}}^M\right\} \quad (10)$$

Equation (10) constitutes the sliding parameters estimation, which can be used instead of equation (2). The convergence of error ϵ can be tuned by the choice of matrix G, which defines the settling times for the observed states. In our application, the matrix G allows to act on two important points:

- Confidence on each measured variable: the choice of the matrix G allows to tune differently each settling time for the state variables (y-lateral deviation and $\tilde{\theta}$-angular deviation). As a result, a more important settling time can be chosen for the less confident measured variable. In our case, the heading measured by the GPS (and then the angular deviation) is derived from a Kalman filter. Therefore, this variable may not be always relevant. The choice made on matrix G will then allow to give more confidence to the measured lateral deviation with respect to the measured angular deviation.
- Noise level on sliding parameters estimated: the settling time of the observer allows to smooth the observed state with respect to the measured one. Consequently, the control variables calculated (i.e. the sliding parameters estimated) are smoothed in the same way. This effect is however limited, as the settling time must be sufficient to preserve the observer convergence.

The observer (10) can then clearly improve the sliding estimation reliability with respect to the direct calculation (2).

IV. EXPERIMENTAL RESULTS

In practice, the sliding parameters provided by the observer are filtered prior to be sent to the main control law. The cut-off frequency of this filter is however higher than the one used on the sliding parameters delivered by equation (2). The delay thus introduced is then quite reduced. As a result, the associated control law is expected to be more reactive.

A. Path to be followed

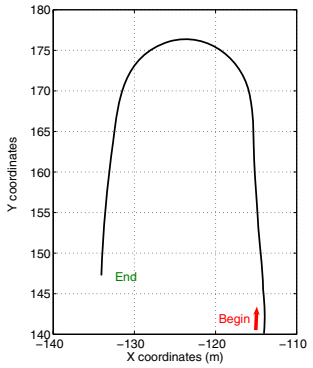

Fig. 4. Path to be followed

A reference path has been recorded by the GPS sensor, while the vehicle was driven manually (the control loop was not active). This path, to be followed in an automatic mode, is depicted on figure 4. It is composed of a straight line, a constant curve, and another straight line. During the tracking of this path, the constant curve will lead to constant sliding conditions for a given duration, longer than the control law settling time. This allows a relevant analysis of the control scheme depicted on figure 3, when sliding conditions are constant. In addition, the beginning and the end of the curve are representative of transient phases for sliding parameters. In all forthcoming experiments, the path has been followed at a constant speed of almost $9km.H^{-1}$, which is consistent with the speeds required in actual agricultural work.

B. Experimental choice for matrix G

During experiments, the matrix G (which specifies the convergence of the observer) has been set to:

$$G = \begin{bmatrix} -2.8 & 0 \\ 0 & -0.8 \end{bmatrix} \quad (11)$$

These settings allow to decouple the behaviour of each variable in the observed state: it ensures a settling time of 1s for the observed lateral deviation and 3.75s for the observed angular deviation. This difference is representative of the important confidence on the measured lateral deviation with respect to the measured angular deviation. At a speed of 9km.H^{-1}, this settling time for the lateral deviation corresponds to a settling distance of 2.7m. It is largely inferior to the settling distance imposed by the control law (**Control2**) (the control gains have been tuned so that the vehicle converges to the reference path within 15m).

C. Sliding estimation and relevance of estimation

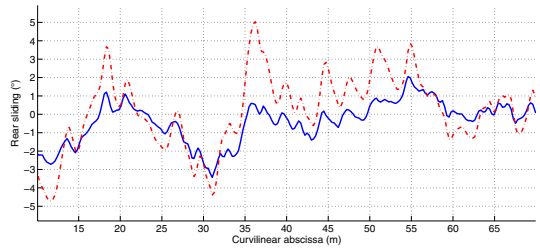

(a) Rear sideslip angles

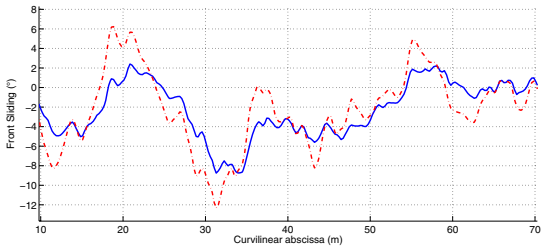

(b) Front sideslip angles

Fig. 5. Sideslip angle observation vs direct calculation

The estimation provided by observer (10) for rear sliding parameter β_P^R (respectively for front sliding parameters β_P^F) is depicted in red dashed line on figure 5 and compared to the parameters calculated with the previous method (2), shown in blue solid line.

It can first be noticed that the level of noise recorded is quite identical, whatever the estimation method considered, although the cut-off frequency of the low-pass filter used in the observer is higher than the one used with the direct calculation. As a consequence, both of them can be injected into the control law with sliding accounted **(Control2)**. Nevertheless, the estimation provided by the observer will be more reactive to variations in sliding conditions.

To appreciate more precisely the differences between the two approaches, sliding parameters resulting either from observer (equation (10)) or directly calculated (using equation (2)) are introduced into model (1) and simulated. Lateral deviations obtained from such simulations should be quite close to the actual lateral deviation recorded. It can be checked on figure 6, where the lateral deviation obtained via the observer is depicted in red dashed dotted line, while the result obtained via the direct calculation method is shown in blue dashed line, and the actual lateral deviation is displayed in black solid line.

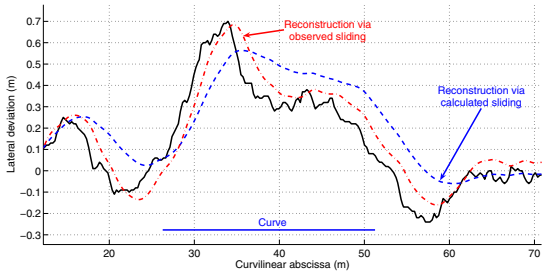

Fig. 6. Comparison of lateral deviation reconstruction

As it could be expected, the deviation obtained from the simulation relying on the observer algorithm is much more closer to the actual deviation. This demonstrates a posteriori that the more important sideslip angles values provided by the observer (shown on figures 5(a)) are more relevant. A delay can still be observed (it is an inevitable effect of low-pass filters), but it has been reduced with respect to the reconstruction supplied by direct calculation.

D. Path following using estimated parameters

The final step consists in achieving path following relying on both estimation algorithms. Actual path tracking errors are compared on figure 7 for the curve following (reference trajectory shown on figure 4) and on figure 8 for a straight line following on a sloping field with a sower on-boarded (as can be seen on figure 2). On these figures, in red dashed dotted line is depicted the tracking error when using **(Control2)** with sliding parameters provided by the observer and in blue dashed line when using the same control law but with the previous estimation algorithm. Finally, the tracking error when using the classical control law **(Control1)** is depicted in black solid line.

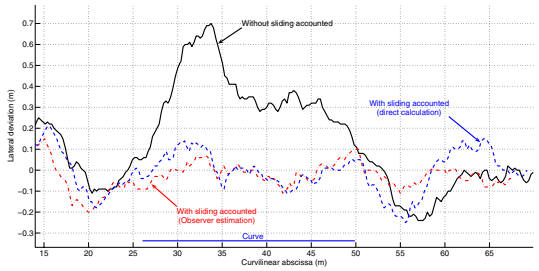

Fig. 7. Comparison of tracking errors in curve with 2 estimation methods

Both tracking errors resulting from the control law with sliding accounted are very close to a null lateral deviation (which is the objective). But it can be noticed that the use of the observer allows to stay closer to zero. It is especially the

case during transient phases (at the beginning and the end of the curve, at curvilinear abscissa 30m and 55m on figure 7). This is a consequence of the shorter settling time provided by the observer. During the line following in slope, the benefit of the observer can clearly be emphasized. In these harsh conditions (terrain irregularities and high level of sliding), the experiment using **(Control2)** with the observer stays very close to zero with only few variations. This is due on one hand, to the reactivity of the observer, already mentioned, and on the other hand, to the difference of confidence introduced in matrix G: in slope, the vehicle heading provided by the Kalman filter is biased, because the vehicle moves crabwise. The experiment using previous sliding estimation shows, on the contrary, numerous and important variations. And finally, the experiment using control law **(Control1)** has an important tracking error (up to 1m).

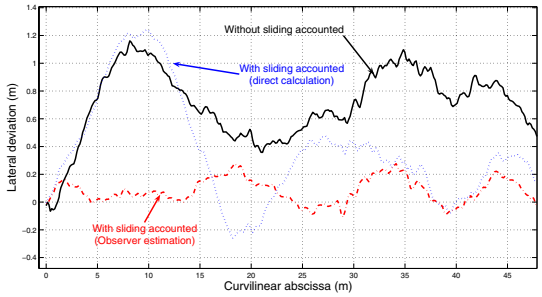

Fig. 8. Comparison of tracking errors in slope with 2 estimation methods

To go further, table V presents the properties (mean, standard deviation and percentage of values within the acceptance range of $\pm$15cm) of each tracking error signal recorded during these experiments. As it can be expected, the results using the control law with sliding accounted are much better than those obtained with the classical control law. Furthermore, the use of the observer allows to reduce considerably the standard deviation and to increase the percentage of values within the acceptance range of $\pm 15cm$ (with respect to direct sliding calculation). It is especially the case in harsh conditions, when sliding parameters change quickly. As a consequence, the tracking errors with the observer stay mainly within a $\pm 15cm$ range of variations, which meets the farmers' expectations.

V. Conclusion and Future Work

This paper proposes an observer-based approach to estimate sliding parameters of an extended kinematic model used to design path tracking control laws for off-road vehicles. The model and the control law have first been recalled. Then the observer design has been detailed, and finally, the relevance of this estimation approach has been investigated through actual experiments and compared to results obtained with the previous method. The benefits of the observer-like estimator for our application (farm tractor achieving path tracking on paddy fields) are pointed out. The tracking error thus obtained stays very close to zero (between $\pm 15cm$ - which meets the farmers' expectations). The accuracy of path tracking in harsh conditions of adherence is improved and more reliable, thanks to a faster reaction, noise reduction and more confidence given to the most relevant measurement.

	mean	std. dev.	% in $\pm$15cm
	During curve		
without sliding	16cm	24cm	38%
direct calculation	-1cm	10cm	84%
with observer	-2cm	7cm	94%
	During slope		
without sliding	67cm	28cm	5.2%
direct calculation	38cm	39cm	23%
with observer	8cm	9cm	75%

TABLE I

Numerical comparison of tracking error in curve

To go further, the integration of dynamic models into observer equations (and not for control purpose) is under study. The aim is to refine the vehicle model in order to account for inertial and three-dimensional effects. Moreover, the developments described in this paper are focused on a sole accurate exteroceptive sensor approach (RTK - GPS). Unfortunately, this sensor is very expensive, which reduces industrialization potential. Current work, carried out jointly with the industrial partner CLAAS, aims at transposing such a global control scheme with several cheaper sensors (decimeter accurate GPS coupled with a gyrometer and an accelerometer). These additional sensors will be also very helpful to supply information to the dynamic models above mentioned.

References

[1] Bornard G., Celle-Couenne F., Gilles G. *Observability and observers*. A.J. Fossard, D. Normand-Cyrot, eds, Chap. 5, Chapman & Hall, 1995

[2] Brunnert A. *Machine Guidance with Laser and GPS.* In Proc. of Conference on Crop Harvesting and Processing, Kentucky (USA), Feb. 2003

[3] Ellouze M., d'Andréa-Novel B. *Control of unicycle-type robots in the presence of sliding effects with only absolute longitudinal and yaw velocities measurement*. In European Journal of Control, 6:567-584, 2000.

[4] Ellouze M., d'Andréa-Novel B. *Tracking with stability for a vehicle braking in a corner*. In Proc. of IEEE Conf. on Decision and Control 5:4427-4432, Orlando, Florida (USA), Dec. 2001

[5] Keicher, R. Seufert, H. *Automatic guidance for agricultural vehicles in Europe* in Computers and Electronics in Agriculture 25(1):169-194, 2000.

[6] Lenain R., Thuilot B., Cariou C., Martinet P. *Model Predictive Control for vehicle guidance in presence of sliding: application to farm vehicles path tracking*. In Proc. of the Intern. Conf. on Robotics and Automation (ICRA), Barcelona, pp. 2546-2551, April 2005.

[7] Micaelli A., Samson C. *Trajectory tracking for unicycle-type and two-steering-wheels mobile robots*. INRIA research report N°2097, Nov. 1993.

[8] O'Connor M., Elkaim G., Bell T., Parkinson B. *Automatic steering of a farm vehicle using GPS*. In Proc. of the 3^{rd} Intern. Conf. on Precision Agriculture, Minneapolis (USA), pp 767-777, June 1996.

[9] Reid J., Niebuhr D. *Driverless tractors*. In Ressource 8(9):7-8, Sept. 2001.

[10] Reid J.F., Zhang Q., Noguchi, N., Dickson, M. *Agricultural automatic guidance research in North America* in Computers and Electronics in Agriculture 25(1):155-167, 2000.

[11] Stentz A., Dima C., Wellington C., Herman H., Stager D. *A system for semi-autonomous tractor operations* in Autonomous robots 13(1):87-104, 2002.

[12] Stephant J, Charara A, Meizel D. *Virtual sensor: Application to vehicle sideslip angle and transversal forces* In IEEE Trans. on Industrial Electronics 53(2):278-289, 2004.

[13] Thuilot B., Cariou C., Martinet P., Berducat M. *Automatic guidance of a farm tractor relying on a single CP-DGPS*. In Autonomous robots 13(1):53-71, July 2002.

[14] The Zodiac. *Theory of robot control*. Canudas de Wit C., Siciliano B. and Bastin G. eds, Springer Verlag, Berlin, 1996.